A&A, 709, L18 (2026)
https://doi.org/10.1051/0004-6361/202660258

Astronomy & Astrophysics

LETTER TO THE EDITOR

Geometric search for Hawking radiation from nearby primordial black holes

Shuo Xiao[1] and Shuang-Nan Zhang[2,3,⋆]

[1] School of Physics and Electronic Science, Guizhou Normal University, Guiyang 550001, PR China
[2] Key Laboratory of Particle Astrophysics, Institute of High Energy Physics, Chinese Academy of Sciences, Beijing 100049, China
[3] University of Chinese Academy of Sciences, Chinese Academy of Sciences, Beijing 100049, China

Received 6 April 2026 / Accepted 26 April 2026

ABSTRACT

A nearby primordial-black-hole (PBH) evaporation burst would produce a curved gamma-ray wavefront, leading to detectable departures from plane-wave inter-satellite delays. We introduce a geometric method that combines imaging localizations with multi-spacecraft timing to determine the distance of a gamma-ray transient. Applied to *Swift*-localized short GRBs, the most constraining event reaches 1.2 AU, already probing a meaningful Solar System-scale regime. Our analysis shows that direct distance measurements are achievable to 10^3 AU scales with the current and near-future technical capabilities. Once a finite source distance is measured, the corresponding PBH mass and lifetime can be directly inferred. Future wide-field localization and long-baseline deep-space gamma-ray detectors could extend such searches to 10^5 AU and beyond.

Key words. methods: analytical – methods: data analysis – methods: observational

1. Introduction

High-energy transient timing analyses universally tend to adopt the plane-wave approximation since the vast majority of gamma-ray bursts (GRBs) have been established as cosmological through afterglows and host associations, and even multimessenger counterparts, as shown in a few cases (Costa et al. 1997; van Paradijs et al. 1997; Piran 2004; Woosley & Bloom 2006; Berger 2014; Kumar & Zhang 2015; Abbott et al. 2017; Goldstein et al. 2017; Savchenko et al. 2017; Li et al. 2018). This approximation underpins multi-spacecraft triangulation and Interplanetary Network (IPN) localizations (Hurley et al. 1999; McClanahan et al. 2011; Svinkin et al. 2022). Nevertheless, it is possible to posit a number of speculative scenarios that could produce nearby, short-duration gamma-ray flashes, including the final evaporation of primordial black holes (PBHs) as a particularly well-motivated example (Hawking 1974; Page 1976; Carr et al. 2010; MacGibbon & Carr 1991; Halzen et al. 1991; Ukwatta et al. 2016; Baker et al. 2025). A nearby burst would imprint a distinctive geometric signature: the incident wavefront is curved and so, arrival-time differences across widely separated spacecraft would end up departing from plane-wave expectations.

Timing-only reconstructions suffer from a fundamental degeneracy, as changes in source direction can mimic changes in distance (Ukwatta et al. 2016). We were able to overcome this limitation by combining imaging localizations with intersatellite timing. Once the sky direction was fixed, the finite-distance problem could be reduced to a single geometric parameter: the source distance. Thus, we were able to formulate, for the first time, a quantitative framework for direct event-by-event distance inference from this combination and apply it systematically to localized short GRBs in current multi-mission data.

This issue is particularly important for PBH searches because the key question in this context is whether a burst is indeed located at a finite, noncosmological distance. Such a regime is astrophysically well motivated: within the Solar System and out to the nearest stellar distances, very few known sources (other than exotic nearby transients) are expected to produce bright millisecond-to-second gamma-ray flashes. Ordinary stellar flares are much slower, while planetary high-energy phenomena such as terrestrial gamma-ray flashes (Fishman et al. 1994) are far too faint to mimic a bright GRB-like event at AU scales. A burst established at such nearby distances would therefore strongly favor a PBH interpretation. Once its distance has been measured, this enables a direct event-by-event physical inference.

2. Data and methodology

2.1. Geometric timing model

Fig. 1 shows the geometric setup. For two detectors i and j at barycentric positions $\mathbf{r}_i$ and $\mathbf{r}_j$, the plane-wave delay for a source from direction $\hat{\mathbf{n}}$ is expressed as

$$\Delta t_{ij}^{\infty} = \frac{\mathbf{B}_{ij}\cdot\hat{\mathbf{n}}}{c}, \qquad \mathbf{B}_{ij} \equiv \mathbf{r}_i - \mathbf{r}_j, \tag{1}$$

where c is the speed of light. For a source at a finite distance D along $\hat{\mathbf{n}}$, the delay becomes

$$\Delta t_{ij}(D) = \frac{|\mathbf{r}_i - D\hat{\mathbf{n}}| - \left|\mathbf{r}_j - D\hat{\mathbf{n}}\right|}{c}. \tag{2}$$

⋆ Corresponding author: zhangsn@ihep.ac.cn

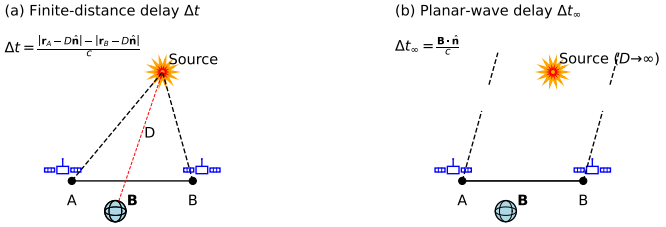

Fig. 1. Geometric test for finite-distance gamma-ray transients. Imaging localization fixes $\hat{\mathbf{n}}$. For a finite distance, D, the delay follows Eq. (2); in the plane-wave limit, it is reduced to Eq. (1). Curvature induces a small deviation scaling as $|\delta t| \propto B_\perp^2/D$, enabling direct geometric distance measurements once the curvature signal is resolved.

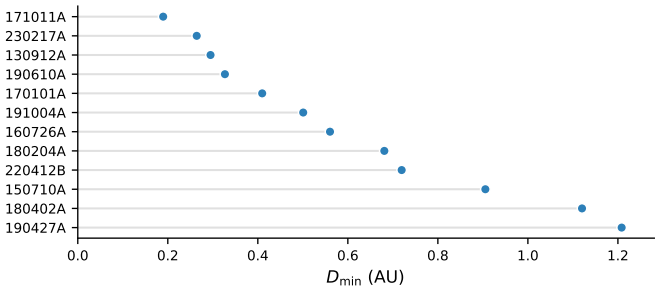

Fig. 2. Distance constraints from the nondetection of wavefront curvature for short GRBs jointly observed by *Konus*-Wind and BAT. Each point shows the conservative 3σ lower limit $D_{\rm min}$ inferred for an individual event. The most constraining case reaches $D_{\rm min} \approx 1.2$ AU, showing that current observations have already entered the Solar System-scale regime relevant to nearby PBH searches. Although the present sample mainly yields lower limits, it has already reached the distance scale at which direct geometric searches for nearby PBH bursts become meaningful.

Once an imaging localization fixes $\hat{\mathbf{n}}$, the problem is reduced to a single parameter, D. Geometrically, a fixed delay defines a two-sheeted hyperboloid with the detectors as foci, while the localization fixes a ray along $\hat{\mathbf{n}}$; the finite-distance solution is their intersection.

For a measured delay $\Delta t_{ij}^{\rm obs}$, Eq. (2) can be inverted analytically. Defining

$$\Delta_{ij} \equiv c\,\Delta t_{ij}^{\rm obs}, \qquad \alpha_i \equiv \hat{\mathbf{n}}\cdot\mathbf{r}_i, \qquad \alpha_j \equiv \hat{\mathbf{n}}\cdot\mathbf{r}_j, \tag{3}$$

the corresponding source distance is

$$D = \frac{\left(|\mathbf{r}_i|^2 - |\mathbf{r}_j|^2\right)(\alpha_i - \alpha_j) - \Delta_{ij}^2(\alpha_i + \alpha_j) \pm \Delta_{ij}\sqrt{Q_{ij}}}{2\left[(\alpha_i - \alpha_j)^2 - \Delta_{ij}^2\right]}, \tag{4}$$

with

$$\begin{aligned} Q_{ij} = {} & |\mathbf{r}_i|^4 + |\mathbf{r}_j|^4 - 2|\mathbf{r}_i|^2|\mathbf{r}_j|^2 - 2\Delta_{ij}^2\left(|\mathbf{r}_i|^2 + |\mathbf{r}_j|^2\right) \\ & + \Delta_{ij}^4 - 4|\mathbf{r}_i|^2\alpha_i\alpha_j + 4|\mathbf{r}_i|^2\alpha_j^2 + 4|\mathbf{r}_j|^2\alpha_i^2 \\ & - 4|\mathbf{r}_j|^2\alpha_i\alpha_j + 4\alpha_i\alpha_j\,\Delta_{ij}^2. \end{aligned} \tag{5}$$

The physical solution is the branch that satisfies Eq. (2) with $D > 0$.

The observed delays, $\Delta t_{ij}^{\rm obs}$, are measured with the modified cross-correlation function (MCCF; Li et al. 1999; Li 2001; Li et al. 2004; Xiao et al. 2021) and uncertainties are estimated from Monte Carlo light-curve realizations. Defining the plane-wave residual $\delta t_{ij} \equiv \Delta t_{ij}^{\rm obs} - \Delta t_{ij}^{\infty}$ and $B_\perp \equiv |\mathbf{B}_{ij} \times \hat{\mathbf{n}}|$, we combine the MCCF uncertainty, σ_{ij}, with localization propagation as

$$\sigma_{ij,\rm tot}^2 = \sigma_{ij}^2 + \sigma_{ij,\rm loc}^2, \qquad \sigma_{ij,\rm loc} \simeq \frac{B_\perp}{c}\,\sigma_\theta, \tag{6}$$

where σ_θ is, for simplicity, the effective but conservatively estimated isotropic localization uncertainty; for events with strongly asymmetric localization regions, a more rigorous treatment would propagate the full two-dimensional localization uncertainty. We can then quantify consistency with the plane-wave hypothesis via $x_{ij} \equiv \delta t_{ij}/\sigma_{ij,\rm tot}$.

For $D \gg |\mathbf{B}_{ij}|$, Eq. (2) yields a curvature correction of order $B_\perp^2/(cD)$, so that the finite-distance deviation scales as $|\delta t| \propto B_\perp^2/D$. Using the conservative bound $|\delta t| \lesssim B_\perp^2/(2cD)$, a null detection at the $k\sigma$ level implies

$$D_{\rm min} \simeq \frac{B_\perp^2}{2c\,k\,\sigma_{ij,\rm tot}}, \qquad (k = 3). \tag{7}$$

What matters physically, however, is not the lower limit itself, but whether the event remains consistent with the infinite-distance limit or, on the other hand, whether it allows for a finite distance scale. Once the curvature signal is resolved above the combined timing and localization uncertainties, Eq. (2) directly yields the source distance and thus distinguishes a nearby burst from an ordinary cosmological GRB.

2.2. Sample and analysis choices

We selected short GRBs ($T_{90} < 3$ s) localized by imaging instruments, focusing on *Swift*/BAT (Sakamoto et al. 2008). We gave priority to bursts without secure redshift or host association, while noting that such events may still be ordinary cosmological GRBs. Our primary demonstration set comes from events jointly observed by *Swift*/BAT and *Konus*-Wind (Aptekar et al. 1995), leveraging the long Wind-Earth baseline for maximal curvature sensitivity. From 44 BAT–KW short GRBs in the considered interval, we selected 12 events with reliable BAT localization, joint detection, and suitable data quality, without any secure redshift or host association.

We measured cross-instrument delays in matched bands and restrict the MCCF to the prompt-emission interval. We also examined near-Earth pairs such as GBM–BAT, GBM–HXMT/HE, and GBM–GECAM as internal consistency checks (Meegan et al. 2009; Zhang et al. 2020; Xiong 2020). Their baselines are far shorter than the Earth-Wind baseline and thus provide much weaker finite-distance constraints.

3. Result

3.1. Plane-wave validation and feasibility of finite-distance identification

For the 12 BAT–KW events in our main sample, all measured delays are shown to be consistent with the plane-wave prediction within 3σ once timing and localization uncertainties are included, showing no significant evidence for wavefront curvature. Near-Earth cross-checks using GBM-BAT, GBM-HXMT/HE, and GBM-GECAM (when available) likewise proved consistent with the plane-wave prediction within 3σ.

In the present sample, the combination of source distances, detector baselines, timing uncertainties, and localization precision means that most events do not yield resolved finite-distance

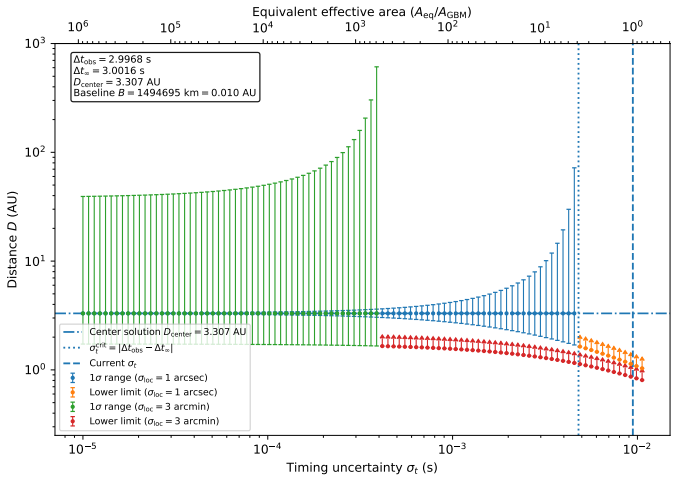

Fig. 3. Distance constraint versus timing uncertainty σ_t for GRB 160726A. Blue points show the central solution and 1σ interval for $\sigma_{loc} = 1$ arcsec, while orange and green points show the corresponding 1σ lower limits for $\sigma_{loc} = 1$ arcsec and 3 arcmin once the upper bound becomes unbounded. The horizontal dash-dotted line marks $D_{center} = 3.307$ AU. The vertical dotted and dashed lines mark $\sigma_t^{crit} = |\Delta t_{obs} - \Delta t_\infty|$ and the current timing uncertainty, respectively. The top axis shows the equivalent effective area relative to GBM. This figure illustrates the threshold at which the method changes from yielding only consistency with the infinite-distance limit to directly measuring a finite source distance.

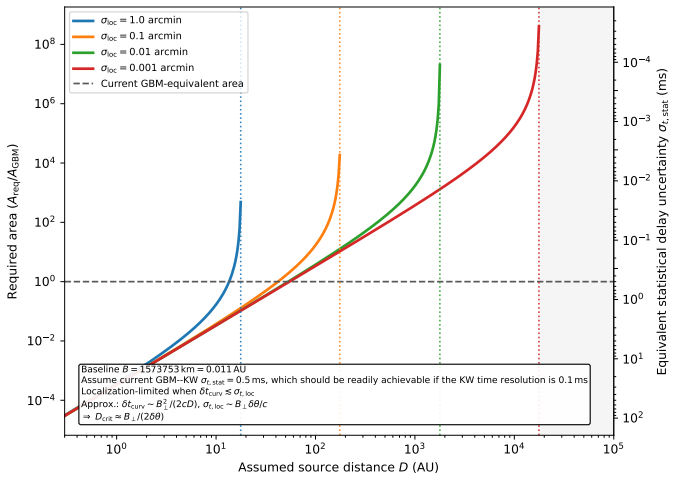

Fig. 4. Required effective area versus assumed source distance for different localization uncertainties. The curves show the equivalent area, in units of the current GBM effective area, required to retain a finite upper bound on the source distance for the GBM–KW baseline. We adopted $\sigma_{t,stat} = 0.5$ ms, consistent with short-GRB timing at a ∼0.1 ms time resolution. The horizontal dashed line marks the current GBM-equivalent area, and the vertical dotted lines mark the critical distances D_{crit} at which the constraint becomes localization-limited. The right axis gives the equivalent statistical delay uncertainty. This figure quantifies how improved timing sensitivity and, in particular, better localization help expand the distance range over which the method can directly measure (rather than merely constrain, the source distance).

solutions. Even so, the most constraining event reaches $D_{min} \approx 1.2$ AU (Fig. 2), showing that current observations have already entered the Solar System-scale regime in which a genuinely finite nearby distance could in principle be identified. This lower bound is not itself the main PBH discriminator; rather, it shows that the method has reached the distance scale where a finite, noncosmological burst distance would become physically meaningful. We emphasize that the present result is a null result: all events remain consistent with the plane-wave approximation within the current uncertainties. A very preliminary Poisson estimate for zero candidate detections gives a local PBH burst-rate limit on the order of $\mathcal{R}_{PBH} \lesssim 0.4\,\mathrm{AU}^{-3}\,\mathrm{yr}^{-1} \approx 3 \times 10^{15}\,\mathrm{pc}^{-3}\,\mathrm{yr}^{-1}$. This estimate is only illustrative, since the present sample is not complete or uniformly selected. The current nondetections therefore reflect the limitations of the available sample and detector configurations, rather than that of the method itself. Our analysis shows that finite nearby distances are already measurable, in principle, from AU to 10^3 AU scales with current capabilities.

3.2. Feasibility of direct geometric distance measurements with future instrumentation

The same geometry also provides a feasibility framework for assessing the future observational conditions required for making direct PBH-inspired distance measurements beyond AU scales. For nearby events, the main challenge is timing; however, at larger distances, the measurement increasingly becomes localization-limited, as illustrated by Figs. 3 and 4. This transition can be characterized by

$$D_{crit} \approx \frac{B_\perp}{2\delta\theta}, \tag{8}$$

where $B_\perp$ is the projected baseline and $\delta\theta$ is the localization uncertainty. Direct distance measurements require the curvature signal to be resolved before this limit is reached. For PBH searches, the physically decisive outcome is therefore not a lower limit by itself, but the identification of a finite, noncosmological distance scale.

This framework also allows an illustrative assessment of how the directly measurable distance range would improve under progressively more capable observational configurations. For a Wind-Earth baseline on the order of $B_\perp \sim 10^6$ km, submillisecond matched-band timing together with arcminute localization, building on the wide-field MPO capability already demonstrated by Einstein Probe/WXT (Yuan et al. 2022), already gives access to distances of order 10 AU (i.e., deep into the Solar System regime). This is essentially achievable with present-day technology: the main limitation is not the baseline itself, but the lack of sufficiently high-time-resolution public products from *Konus*-Wind. Improving the localization by one order of magnitude, to ∼0.1 arcmin (as expected for a next-generation MPO) would push the same baseline toward the 10^2 AU regime, beyond which the measurement would increasingly become localization limited, as indicated by Fig. 4. Even without such an improvement, extending the baseline to Sun–Earth scales, while retaining an arcminute localization would already push the directly measurable distance range to the order of 10^3 AU.

Longer baselines then open a much greater search volume. For instance, for $B_\perp$ on the order of 1 AU, a Mars–Earth configuration combined with ∼0.1 arcmin localization could extend the directly measurable distance range to 10^4 AU, making Mars missions especially attractive opportunities for piggyback gamma-ray detectors. An even more powerful configuration would use Sun–Earth-scale baselines together with a new generation of wide-field instruments reaching arcsecond localization; in that case, the localization-limited reach can approach or exceed 10^5 AU. Since both Mars and solar missions are likely to continue internationally, they offer realistic opportunities to push

purely geometric PBH searches far beyond the current AU-scale frontier.

In practice, σ_t is statistics driven for background-dominated short transients, with $\sigma_t \propto \mathrm{SNR}^{-1} \propto A_{\mathrm{eff}}^{-1/2}$ for comparable backgrounds and bandpasses. This motivates both larger effective area and lower background on millisecond timescales. We adopted $\sigma_{t,\mathrm{stat}} = 0.5\,\mathrm{ms}$, motivated by short-GRB timing performance at ∼0.1 ms resolution (Xiao et al. 2021, 2022). Absolute timing is already adequate for this program: near-Earth missions provide µs–100 µs absolute timing accuracy and µs–sub-µs event time tagging (Meegan et al. 2009; Liu et al. 2020; Xiao et al. 2022), well below the statistical delay uncertainties relevant here. For *Konus*-Wind, the main limitation is typically the publicly available light-curve binning rather than clock accuracy (Aptekar et al. 1995). Thus, the principal technological drivers are no longer clock performance, but wide-field localization accuracy, high-time-resolution data products, along with access to long baselines.

A central advantage of the geometric approach is that, once a finite source distance, D, has been established for a candidate event, the observed energy flux, F, immediately gives the intrinsic luminosity, $L = 4\pi D^2 F$. Based on the interpretation that the burst is Hawking radiation from a nonrotating PBH and defining $F_{-6} \equiv F/(10^{-6}\,\mathrm{erg\,cm^{-2}\,s^{-1}})$, as the typical peak flux of a short GRB), the corresponding PBH mass is

$$M \simeq 1.13 \times 10^{11} \left(\frac{D}{100\,\mathrm{AU}}\right) F_{-6}^{-1/2}\,\mathrm{kg}. \tag{9}$$

The corresponding PBH lifetime from formation to final evaporation is then

$$\tau \simeq 3.80 \times 10^{9} \left(\frac{D}{100\,\mathrm{AU}}\right)^{3} F_{-6}^{-3/2}\,\mathrm{yr}. \tag{10}$$

Thus, unlike rate-based searches, a geometric distance measurement would provide direct event-by-event access to the PBH mass and lifetime under the Hawking-burst interpretation (Hawking 1974, 1975). A finite-distance measurement without a counterpart would identify a nearby transient, but PBH identification would still require spectral and temporal consistency checks against theoretical predictions of a Hawking-burst. It is interesting to note that for $\tau \sim 1.37 \times 10^{10}$ yr, i.e., the age of the universe, we have $D \sim 150$ AU for a typical short GRB. This is clearly within the reach of an AU scale baseline with current wide-field X-ray imaging and gamma-ray timing capabilities.

4. Conclusion

We introduce a geometric method for measuring the distance of nearby gamma-ray transients that combines imaging localizations with multi-spacecraft timing. Applied to localized short GRBs without redshift, the current sample shows no evidence for wavefront curvature and remains consistent with the plane-wave approximation across missions. This reflects the limitations of the presently available events and detector configurations, rather than any limitation of the method itself.

The main result is that AU-scale direct distance measurements are already feasible in principle with current or near-future capabilities. What matters physically is not the lower limit itself, but the question of whether the event can be shown to lie at a finite, noncosmological distance. Such a result would immediately distinguish the burst from ordinary cosmological GRBs and would strongly point to an exotic nearby origin, such as PBH evaporation. Because few known astrophysical sources are expected to produce bright millisecond-to-second gamma-ray flashes within the Solar System and its neighborhood, systematic searches for such nearby events are already well motivated.

Figures 3 and 4 summarize the key requirements for extending this capability. Wind-Earth-scale baselines with an arcminute-to-subarcminute localization already reach from 10 to 10^2 AU, while Sun-Earth-scale baselines with an arcminute localization can already extend the directly measurable range to 10^3 AU. Furthermore, Mars-Earth configurations combined with ∼0.1 arcmin localization can further extend the reach to 10^4 AU, while Sun-Earth-scale baselines combined with arcsecond localization could push direct geometric searches toward 10^5 AU. Taken together, these advances provide a realistic roadmap from the current AU-scale regime to much larger search volumes for nearby PBH bursts.

Acknowledgements. We acknowledge the use of public data from *Fermi*/GBM, *Konus*-Wind, *Swift*, *Insight*-HXMT, and GECAM. This work is supported by the National Natural Science Foundation of China (Nos. 12303043, 12333007 and 12573043), Science and Technology Foundation of Guizhou Province (Key Program, Nos. [2025]021 and ZK[2024]430), and the Space Origins Program of the Chinese Academy of Sciences.

References

Abbott, B. P., Abbott, R., Abbott, T., et al. 2017, ApJ, 848, L13
Aptekar, R., Frederiks, D., Golenetskii, S., et al. 1995, Space Sci. Rev., 71, 265
Baker, M. J., Iguaz Juan, J., Symons, A., & Thamm, A. 2025, Phys. Rev. Lett., 135, 111002
Berger, E. 2014, ARA&A, 52, 43
Carr, B. J., Kohri, K., Sendouda, Y., & Yokoyama, J. 2010, Phys. Rev. D, 81, 104019
Costa, E., Frontera, F., Heise, J., et al. 1997, Nature, 387, 783
Fishman, G. J., Bhat, P. N., Mallozzi, R., et al. 1994, Science, 264, 1313
Goldstein, A., Veres, P., Burns, E., et al. 2017, ApJ, 848, L14
Halzen, F., Zas, E., MacGibbon, J. H., & Weekes, T. C. 1991, Nature, 353, 807
Hawking, S. W. 1974, Nature, 248, 30
Hawking, S. W. 1975, Commun. Math. Phys., 43, 199
Hurley, K., Briggs, M. S., Kippen, R. M., et al. 1999, ApJS, 122, 497
Kumar, P., & Zhang, B. 2015, Phys. Rep., 561, 1
Li, T. P. 2001, Chin. J. Astron. Astrophys., 1, 313
Li, T. P., Feng, Y., & Chen, L. 1999, ApJ, 521, 789
Li, T. P., Qu, J.-L., Feng, H., et al. 2004, Chin. J. Astron. Astrophys., 4, 583
Li, T., Xiong, S., Zhang, S., et al. 2018, Sci. China: Phys. Mech. Astron., 61, 031011
Liu, C., Zhang, Y., Li, X., et al. 2020, Sci. China: Phys. Mech. Astron., 63, 1
MacGibbon, J. H., & Carr, B. J. 1991, ApJ, 371, 447
McClanahan, T. P., Hurley, K., Briggs, M. S., et al. 2011, ApJS, 196, 1
Meegan, C., Lichti, G., Bhat, P. N., et al. 2009, ApJ, 702, 791
Page, D. N. 1976, ApJ, 206, 1
Piran, T. 2004, Rev. Mod. Phys., 76, 1143
Sakamoto, T., Barthelmy, S., Barbier, L., et al. 2008, ApJS, 175, 179
Savchenko, V., Ferrigno, C., Kuulkers, E., et al. 2017, ApJ, 848, L15
Svinkin, D. S., Hurley, K., Ridnaia, A. V., et al. 2022, ApJS, 259, 34
Ukwatta, T. N., Hurley, K., MacGibbon, J. H., et al. 2016, ApJ, 826, 98
van Paradijs, J., Groot, P. J., Galama, T., et al. 1997, Nature, 386, 686
Woosley, S. E., & Bloom, J. S. 2006, ARA&A, 44, 507
Xiao, S., Xiong, S. L., Zhang, S. N., et al. 2021, ApJ, 920, 43
Xiao, S., Liu, Y., Peng, W., et al. 2022, MNRAS, 511, 964
Xiong, S. 2020, Sci. Sin. Phys. Mech. Astron., 50, 129501
Yuan, W., Zhang, C., Feng, H., et al. 2022, Proc. SPIE, 12181, 1218112
Zhang, S.-N., Li, T., Lu, F., et al. 2020, Sci. China: Phys. Mech. Astron., 63, 1